EFFECT OF AGING, TEMPERATURE, AND AMBIENT GASES ON THE COMPLEX IMPEDANCE OF $As_2Te_{13}Ge_8S_3$ GLASSY FILMS

Marina Ciobanu* and Dumitru Tsiulyanu

CIMAN Research Centre, Department of Physics, Technical University of Moldova, Chisinau, MD-2060 Republic of Moldova,
**E-mail: ciobmarina@gmail.com*

(Received October 18, 2021)

https://doi.org/10.53081/mjps.2021.20-2.06 CZU:539.2:538.9

Abstract

The work is focused on the application of the impedance spectroscopy method to provide evidence and study the effects of aging, temperature, and gas adsorption in chalcogenide-based thin films. The experiments are carried out with thin films of glassy quaternary composition $As_2Te_{13}Ge_8S_3$ in a wide frequency range at different temperatures under different environmental conditions, in particular, either dry or wet air or their mixtures with NO_2 or CO_2. It is found that aging has a significant effect on the impedance spectra of Pt–$As_2Te_{13}Ge_8S_3$–Pt functional structures, which make evidence for the presence of substantial spatial and compositional disordering. This effect can be stabilized by the post-preparation annealing of the sample. The effect of temperature on impedance spectra consists in a variation in the both real and imaginary parts of impedance that appear to be extremely sensitive to adsorptive processes. Adsorption of nitrogen dioxide results in a significant frequency-dependent decrease in the impedance parameters, which is attributed to an effective “strong” chemisorption process due to the interaction of "odd" electrons of NO_2 molecules with lone pair electrons of chalcogen atoms. The effect of water vapors leads only to an increase in the real part of impedance, while the imaginary part abruptly decreases; this fact is attributed to a “weak” form of chemisorption. The effect of carbon dioxide on the impedance spectra is attributed to the physical adsorption of CO_2 molecules. This effect is weak; however, it is reversible and clearly observed even at room temperature.

Keywords: chalcogenides, impedance, aging, adsorption, NO_2, CO_2

Rezumat

Lucrarea este dedicată aplicării metodei de spectroscopie a impedanței pentru a oferi dovezi și investigații ale influenței îmbătrânirii, temperaturii și adsorbției gazelor în pelicule subțiri pe bază de calcogenuri amorfe. Experimentele au fost efectuate cu filme subțiri cuaternare sticloase $As_2Te_{13}Ge_8S_3$ într-o gamă largă de frecvențe, la diferite temperaturi și condiții ambiante, inclusiv aer uscat sau umed, precum și amestecurile lor cu NO_2 sau CO_2.Sa constatat o influență avansată a îmbătrânirii asupra spectrelor de impedanță ale structurilor funcționale Pt -

$As_2Te_{13}Ge_8S_3$ - Pt, cea ce confirmă prezența unei dezordine spațiale și compoziționale mari ale structurii. Această influență poate fi stabilizată prin tratarea termică a eșantionului. Influența temperaturii asupra spectrelor de impedanță constă în variația părților reale și imaginare ale impedanței care sunt foarte sensibile la procesele de adsorbție. Adsorbția dioxidului de azot, dependent de frecvența câmpului electric aplicat, aduce la o scădere esențială a parametrilor impedanței, ceea ce se explică printr-un proces de chemosorbție „puternic" eficient datorat interacțiunii electronilor „neobișnuiți" ai moleculelor de NO_2 cu perechile de electronii solitari ale atomilor de calcogen. Adsorbția vaporilor de apă duce doar la creșterea părții reale a impedanței, pe când partea sa imaginară descrește brusc, explicată printr-o formă „slabă" de chemisorbție. Efectul dioxidului de carbon asupra spectrelor de impedanță este explicat prin adsorbția fizică a moleculelor de CO_2. Acest efect este slab, dar este reversibil și clar observat chiar și la temperatura camerei.

Cuvinte cheie: calcogenuri, impedanță, îmbătrânire, adsorbție, NO_2, CO_2

1. Introduction

The unique properties of glassy and amorphous chalcogenides, which have determined the wide application of these materials in micro and optoelectronics [1], are attributed to their special chemistry and defect states, caused by structural and compositional disordering. On the other hand, the disordering does not allow using the conventional modern methods, in particular, SEM and XRD, to reveal and study the physical and chemical processes that occur under the action of natural or induced factors, such as aging, annealing, irradiation, and adsorption. In this respect, impedance spectroscopy appears to be an indirect, yet extremely sensible method to provide evidence and study the effect of these external factors on disordered materials, in particular, glassy and amorphous films. The spectral distribution of impedance provides extensive information about the electrical properties of the electrode- material system and the electrophysical processes that occur in it [2]. At the beginning, the impedance measurements have been successfully applied to study the effects of aging, temperature, and NH_3 adsorption on micro and nanocrystalline tellurium-based thin films [3, 4].

Later, the impedance spectra of amorphous tellurium films by adsorption of other gases (NO_2, H_2S, H_2) were studied; moreover, an attempt was made to elucidate the effect of the glassy material composition on the spectral distribution of impedance in a complex (Nyquist) plot, under the application of nitrogen dioxide at room temperature [5]. As a result, a model of gas (NO_2)–chalcogenide solid interaction has been proposed and the possibility of using glassy chalcogenide (GCh) films for the development of low-temperature impedance operating gas sensitivity devices has been pointed out. The impedance sensitivity of $As_2Te_{13}Ge_8S_3$ quaternary glassy films was shown to be the highest among the tested compositions; this finding was attributed to the highest spatial and compositional disordering of the surface of these films. The high sensitivity to toxic gases makes this material attractive for detecting low reactive gases, such as carbon dioxide. The carbon dioxide molecule is an extremely stable and low reactive molecule [6]. To date, various materials have been studied to detect carbon dioxide, such as thick layers of $BaTiO_3$ [7], thin films of CdSe [8] or In_2Te_3 [9]; however, in all cases, the operating temperature is high. In this work, we have tried to detect carbon dioxide at room temperature using highly sensitive glassy quaternary chalcogenide materials $As_2S_3Ge_8$–Te via the impedance spectroscopy method. Due to

the high disordering of $As_2S_3Ge_8$–Te films and their possible chronological degradation, the effects of aging and temperature on complex impedance spectra have been studied first.

2. Materials and Methods

The $As_2Te_{13}Ge_8S_3$ quaternary composition was synthesized using pure (99.9%) As, S, Te, and Ge. The synthesis was performed by conventional melt-quenching in a vacuum of 5×10^{-5} Torr at 900°C for 24 h. The ampoule was agitated for homogenization during the synthesis and then quenched on a copper refrigerator with running water. Thin films based on the synthesized material were grown by thermal "flash" evaporation in a vacuum onto sintered alumina substrates with predeposited interdigital Pt electrodes at an electrode width of 15 μm and interelectrode distances of 45 μm (Fig. 1a). The growth velocity of the film was 30 nm/s; however, the film thickness was about 60 nm, being assessed using a MII-4 micro interferometer. The surface morphology of the films was studied with a VEGA TESCAN TS 5130 MM scanning electron microscope (SEM); X-ray diffraction (XRD) analysis was performed using a DRON-YM1 diffractometer. Impedance measurements were carried out in a frequency range of 5 Hz to 13 MHz at a probing signal level of 100 mV using an HP4192A impedance analyzer (Agilent Technologies, United States). The measurements were carried out at different temperatures in either dry or wet air or their mixtures with a NO_2 vapor. The NO_2 vapor with a concentration of 1.5 ppm was obtained by using a calibrated permeation cylinder (Vici Metronics, United States), which was incorporated into the experimental setup described in detail in our previous paper [10]. The carrier gas was humidified using a saturated solution of the NaBr salt in water, which is known to give a controlled relative humidity of 58%. Carbon dioxide diluted in dry air with a calibrated concentration of 1.0 vol % was obtained from cylinders (Linde, Germany). For all experiments, the thin film devices were put into a test cell (volume of 10 mL), in which the gases were injected parallel to the film surface. A constant flow (100 mL/min) was maintained by mass flow controllers (Wigha, Germany). A PT-100 platinum resistance temperature detector (Cliptec Kabeltechnik, Germany) close to the film was used for assisting the temperature control.

3. Results

3.1. X-ray diffraction and SEM measurements

Figure 1(b) shows a SEM image of a chalcogenide film grown on a simple substrate (without predeposited Pt electrodes). It is evident that the film consists of agglomerated interconnected islands, which are responsible for the high surface roughness of the film. No crystallite tracks are observed. The amorphous state of the film was confirmed also by the XRD measurements performed using the FeK_α radiation at a rotation velocity of the scintillation counter of 2 or 4 deg/min. The XRD pattern of an $As_2Te_{13}Ge_8S_3$ quaternary film deposited on sintered alumina (Al_2O_3) substrates is shown in Fig. 1c. The pattern does not comprise any XRD peaks, which gives evidence that the $As_2Te_{13}Ge_8S_3$ films are in the amorphous state.

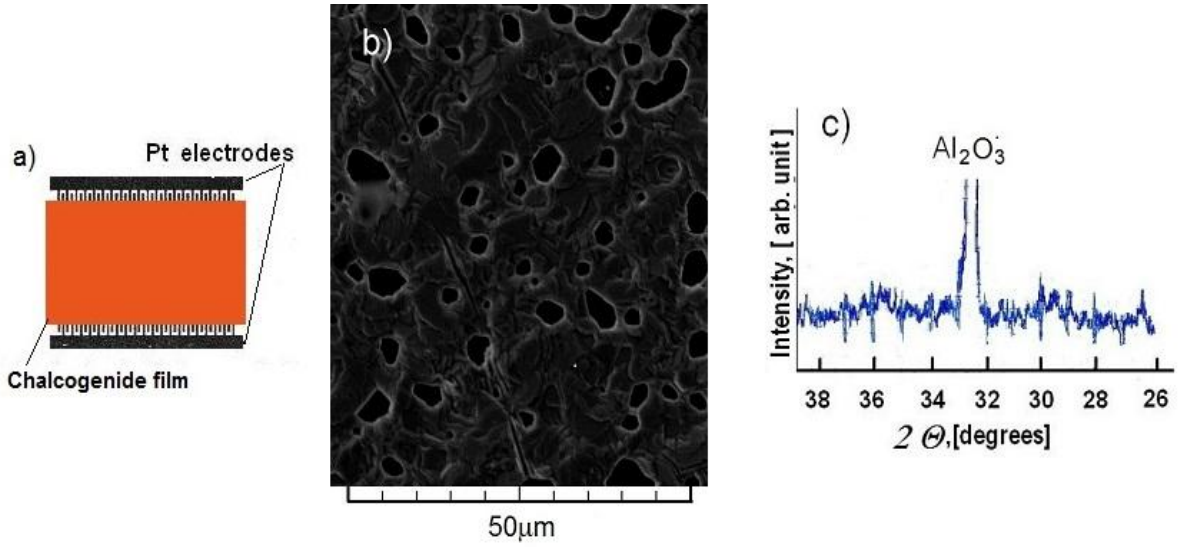

Fig. 1. (a) Schematic representation of the experimental sample, (b) SEM image, and (c) XRD pattern of $As_2Te_{13}Ge_8S_3$ thin films grown onto sintered alumina substrates (adapted from [10]).

3.2. Effect of aging on complex impedance spectra

Figure 2 shows a typical complex impedance diagram in the Nyquist plot obtained in dry air from the as-grown and aged (at different durations) $As_2Te_{13}Ge_8S_3$ based thin film device at room temperature (22°C). It is evident that the diagram of a virgin film represents a semi arc. No displacements of the center of the arc relative to the real axis are observed; this fact indicates the homogeneity of the chalcogenide material and the absence of other distributed elements in the considered thin film devices [2].

At the same time, it can be observed that this arc is not a perfect semicircular arc due to its stretching at low Re(Z) values, i.e., at high frequencies of the applied field. Thus, the considered Nyquist plot can be interpreted by a simplified equivalent circuit (inserted in Fig. 2), which consists of frequency dependent resistance R_ω and capacitance C_ω connected in parallel. Aging at room temperature leads to an increase in the radius of the arc, so much that, after 8 months, the values of the imaginary part of the impedance exceed the measuring limits of the analyzer device. At the same time, it is clearly obvious from Fig. 2 that the aging effect is saturated. Moreover, the effect of aging can be eliminated via annealing of the samples after preparation. Figure 2 shows that annealing at 50^{o}C for 2 h stabilized the aging evolution.

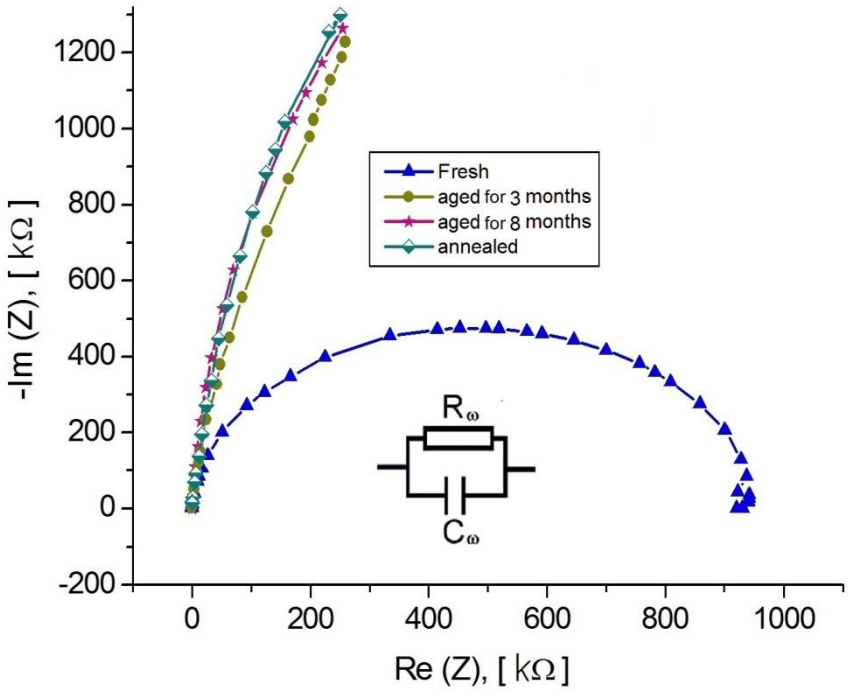

Fig. 2. Impedance spectra at 22°C in dry air of the as-grown and either annealed or aged (at different durations) chalcogenide based $As_2Te_{13}Ge_8S_3$ films. The insert shows the equivalent circuit used for analysis.

3.3. Temperature effect

The effect of temperature on impedance spectra was studied using films presaged for 8 months. Figure 3 shows the complex impedance spectra of $As_2Te_{13}Ge_8S_3$ films under dry air versus temperature. It is evident that heating leads to a variation in both the real and imaginary part of the impedance due to a variation in the frequency-dependent resistance and capacitance of the thin film device. Due to the limitation imposed by the used impedance analyzer, the characteristic frequency f_m, that is, the frequency at which the imaginary part reaches its maximum value, cannot be reached in the given temperature range. Accordingly, the resistance R_m and capacitance C_m at the characteristic frequency f_m that characterizes the complex impedance spectra cannot be determined. Therefore, we estimated the temperature effect on resistance and capacitance at a frequency of 13 kHz, which is the lowest frequency allowing not exceeding the limits of the analyzer. The inset in Fig. 3 shows the effect of temperature on both the resistance and capacitance of the Pt–$As_2Te_{13}Ge_8S_3$–Pt functional structure in dry air at 13 kHz.

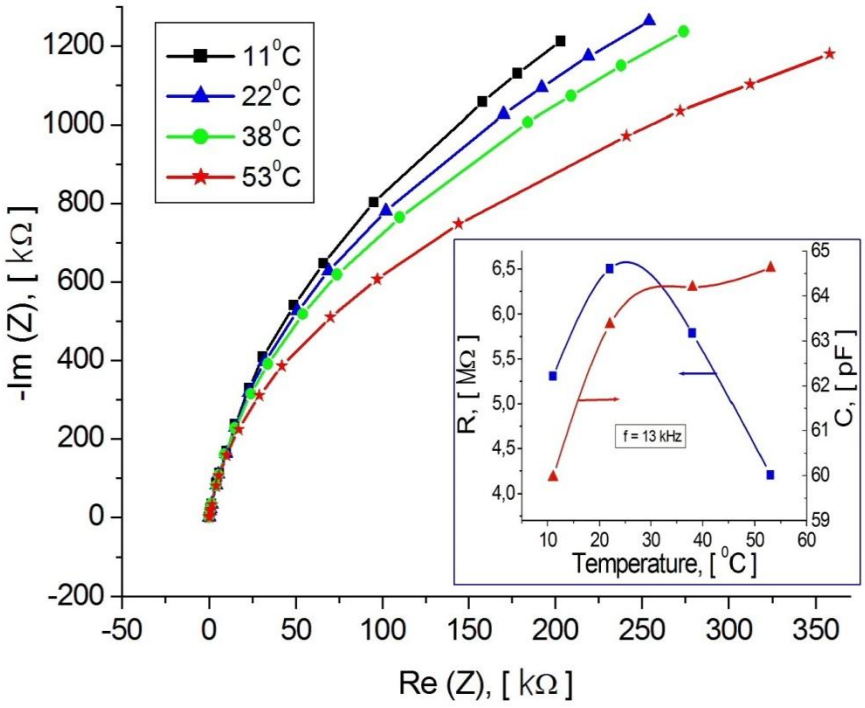

Fig. 3. Effect of temperature on the complex impedance spectra of $As_2Te_{13}Ge_8S_3$ films. The inset shows the temperature dependence of resistance and capacitance at a frequency of 13 kHz.

3.4. Effect of gas adsorption

3.4.1. Nitrogen dioxide and water vapors

Figure 4 shows the effect of nitrogen dioxide on impedance spectra of the aged $As_2Te_{13}Ge_8S_3$ thin films at room temperature. It is evident that the use of extremely low concentrations (ppm) of NO_2 significantly diminishes the radius of the Nyquist arc in such a way that even the characteristic frequency can be estimated as $f_m \approx 4$ kHz. The values of the real and imaginary parts of the impedance and the time constant $\tau_m = (2\pi f_m)^{-1}$ are 755 kΩ, 682 kΩ, and 4×10^{-5} s, respectively. To estimate the effect of NO_2 adsorption, the variation in both the real and imaginary parts of the impedance was calculated as $\Delta X = X_{air} - X_{NO_2}$, where X is either Re(Z) or Im(Z) at a frequency of 13 kHz, which is the frequency at which all parameters can be measured. The diagram inserted in Fig. 4 shows the effect of nitrogen dioxide on the real and imaginary parts of impedance. It is evident that the adsorption of nitrogen dioxide vapors leads to a decrease in both the real and imaginary part of the impedance; however, the decrease in the imaginary part is huge: approximately 100 times higher than that of the real part.

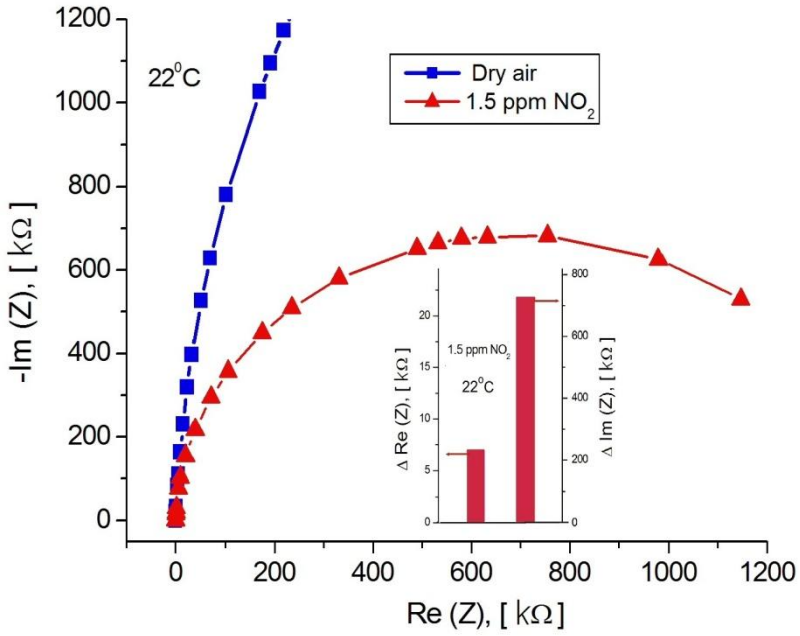

Fig. 4. Effect of NO_2 on complex impedance spectra of $As_2Te_{13}Ge_8S_3$ films at room temperature. the insert shows the variation in both the real and imaginary parts of the impedance at 13 kHz.

The effect of the water vapor on the complex impedance spectrum appears to be opposite to that of the nitrogen dioxide: the adsorption of water vapors leads to an increase in the radius of the Nyquist arc. Figure 5 shows the complex impedance spectra of the functional Pt–$As_2Te_{13}Ge_8S_3$–Pt structure in both dry and wet (58% RH) air. The increase in the radius of the Nyquist arc is attributed to a variation in both the real and imaginary parts of the impedance. Unlike the effect of NO_2 vapors, in the given frequency range, only the real part of the impedance slightly increases with air humidification; the imaginary part significantly diminishes. The inset in Fig. 5 shows the variation in both the real and imaginary parts of the impedance at 13 kHz with the humidification of air at room temperature to 58% RH. It is observed that the real and imaginary parts of the impedance vary in opposite directions; however, the increase in the imaginary part is much more significant than the decrease in the real part.

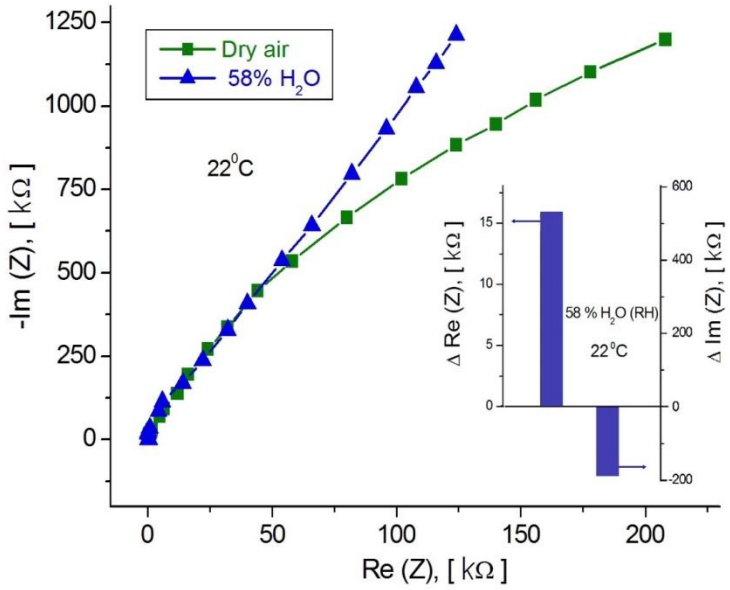

Fig. 5. Effect of water vapors on complex impedance spectra. The inserted diagram shows the variation in both the real and imaginary parts of the impedance at 13 kHz upon the humidification to 58% RH.

As the interfering effect of the water vapor with NO_2 ones is concerned, it is worth noting that it is not so essential. Even at room temperature, the 58% RH increases the impedance by 30–200 kΩ and thereby diminishes the effect of NO_2 by not more than 15%.

3.4.2. Carbon dioxide

Figure 6 shows the complex spectra of the impedance of the Pt–$As_2Te_{13}Ge_8S_3$–Pt functional structure in dry air and in the case of using 1 vol % CO_2 and subsequently removing it. It is observed that the effect of CO_2 vapors on the complex impedance spectra is similar to the effect of water vapors, although it is much weaker: depending on frequency, the real part of the impedance decreases and the imaginary part increases. After the removal of CO_2, the frequency-dependent impedance almost completely recovers.

The insert in Fig. 6 shows the variation (differences) in both the real and imaginary part of the impedance upon switching from pure dry air to its mixture comprising CO_2 as the target gas. This diagram makes it possible to compare the effects of CO_2 and water vapors on the impedance of the functional structure under study. It is evident from the diagrams inserted in Figs. 5 and 6 that the main difference between the effects of these two target gases consists in the high difference in the variation of the imaginary part of the impedance: at 13 kHz, Im(Z) vary by approximately 200 kΩ for water vapors and as low as by 8 kΩ for CO_2 vapors.

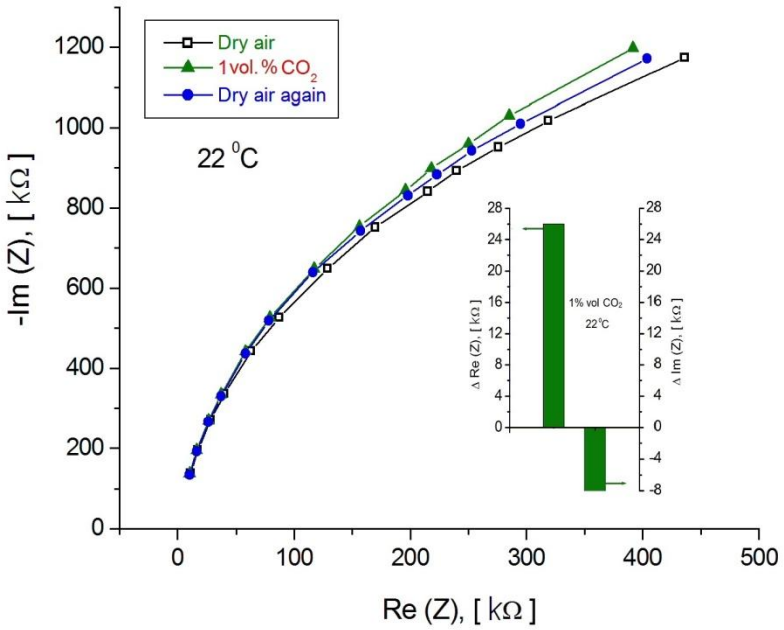

Fig. 6. Effect of CO_2 vapors on the complex impedance spectra of quaternary chalcogenide films $As_2Te_{13}Ge_8S_3$ at room temperature. The inset shows the variation in both the real and imaginary part of the impedance due to the application of CO_2 at 13 kHz and room temperature.

4. Discussion

The features of complex impedance spectra of GChes, in particular, $As_2Te_{13}Ge_8S_3$ quaternary films are obviously attributed to the specific features of this class of materials [11]. Being covalent semiconductors, they exhibit a lack of long-range order of the structure, which results in a random fluctuation of potential, tailing of band edges, and localization of these tail states. In addition, these materials are representatives of so called lone-pair (LP) semiconductors, which contain a large concentration of group V and VI elements of the periodic table. The main specific feature of LP semiconductors is that the LP orbitals form the upper part of the valence band. If the network contains defects, such as unsaturated chemical bonds (dangling bonds), the interaction between these defects and the LP electrons occurs. The dangling bond interacts with the neighboring LP to bond with it by distorting its environment [12]. This interaction results in the release of about 10^{13}–10^{15} holes/cm^3 and causes the *p*-type of conductivity. Thus, the spatial and compositional disordering, as well as the special chemistry and defect states, leads to interesting—sometimes unique—properties of GChes. In this context, the effect of aging on the complex impedance spectra of $As_2Te_{13}Ge_8S_3$ films (Fig. 2) can be attributed to the self-reconstruction of the spatial random network. At the same time, the stretching of the Nyquist arc at high frequencies of the applied field, i.e., at low Re(*Z*) values, becomes explicable taking into consideration the specific features of the charge transport in disordered materials [11], in particular, quaternary$As_2Te_{13}Ge_8S_3$ under study [10]. AC conductivity at high frequencies implies not only the conventional transport via extended states above mobility edges, but also the

hopping transport via localized states in the gap, in particular, the states at the Fermi level.

Heating results in a variation in both the real and imaginary part of impedance due to a variation in the frequency-dependent resistance and capacitance of the thin film device. From simple analysis of the equivalent circuit, the R_ω and C_ω values of the film were evaluated as follows:

$$R_\omega = \frac{\mathrm{Im}^2(Z) + \mathrm{Re}^2(Z)}{\mathrm{Re}(Z)} \quad (1), \qquad C_\omega = \frac{\mathrm{Im}(Z)}{\omega\left[\mathrm{Im}^2(Z) + \mathrm{Re}^2(Z)\right]} \quad (2)$$

The effect of temperature on the resistance of the Pt–$As_2Te_{13}Ge_8S_3$–Pt functional structure, which is shown in the insert in Fig. 3, indicates that, at 13 kHz, the resistance initially (up to 22°C) increases and then decreases according to the conventional semiconductor behavior. This behavior was observed earlier in pure Te films [3]; it was attributed to the effect of the adsorption–desorption processes of molecular oxygen from the carrier gas, i.e., dry air. Although the physisorption and/or "weak" chemisorption of O_2 molecules diminishes the resistance of the GCh, at each temperature, a competition between the rates of its adsorption and desorption occurs. Thus, up to 22°C (first step), the resistance increases because of the fast desorption of prephysisorbed oxygen and then decreases owing to the semiconductor properties of $As_2Te_{13}Ge_8S_3$, that is, the conductivity exponentially increases with an increase in temperature [13]. Apparently, the desorption process affects the capacity of the GCh-based functional structure as well. The insert in Fig. 3 shows a significant increase in capacitance with an increase in temperature up to 22°C; at higher temperatures, this increase is much slower. In the last-mentioned case, the frequency-dependent capacitance becomes controlled only by semiconductor band bending at the surface [14].

Nitrogen dioxide is known to be highly chemisorbed by chalcogenide glasses [15–17]. Chemisorption of NO_2 leads to the formation of acceptor levels because its molecule comprises an odd (unshared) electron [6], which can accept a LP electron from a ChG atom to form a chemical bond and release an additional hole at the surface. As a result, both the surface band bending and electrical conductivity increase. Thus, the decrease in the impedance parameters during NO_2 adsorption (Fig. 4) is due to an increase in the hole density in the accumulation (surface) region.

The effect of water vapors can be attributed to a "weak" chemisorption of H_2O molecules. It was shown in [18] that the adsorption of H_2O molecules diminishes the DC conductivity of the film; however, it leads to an increase in the work function change of the GCh. The last-mentioned fact is associated with the effect of the dipole component of the work function, which arises from the formation of a double electric layer on the surface. The water molecules exhibit a high ($15 \cdot 10^{-30} C \cdot m$) dipole moment; therefore, while approaching the surface of a positively charged GCh film, they rotate and orientate their dipole moments perpendicular to this surface with a negative pole inward. At the same time, the free lattice holes become more and more localized at the points of the surface increasing the real part of the impedance. At the same time, the preferential alignment of the water dipoles affets the double charged layer at the surface, which results in a noticeable decrease in the imaginary part of the impedance (see the insert in Fig. 5). Thus, the effect of water vapors is attributed to the orientation polarization of H_2O molecules on the surface and the formation of weak bonds with an electrostatic origin, the so-called "weak" form of chemisorption [19].

Unlike H_2O molecules, the gaseous carbon dioxide molecule has a symmetric shape and

has no permanent dipole moment. In addition, it is an extremely stable molecule, which can dissociate only at temperatures higher than 2000^{o}C. These features hinder the detection of this pollutant gas at temperatures that are not high, especially, at room temperatures. Nevertheless, the impedance spectra of chalcogenide-based functional structures under study exhibit an evident sensitivity to CO_2 via a slight and reversible increase in the real part of impedance accompanied by a decrease in its imaginary part. We assume that this phenomenon occurs due to a simple physisorption caused by the deformation polarization of CO_2 molecules approaching the charged surface of the GCh, which affects the mobility of free holes in the accumulation region adjacent to the surface.

5. Conclusions

The impedance spectroscopy is an effective extremely sensible method to reveal the effect of aging, heating, and gas adsorption on disordered chalcogenide films. The evolution of the impedance spectra of Pt–$As_2Te_{13}Ge_8S_3$–Pt functional structures under aging makes evidence for the presence of a significant spatial and compositional disordering of the chalcogenide film that can be stabilized by the post-preparation annealing of the sample. The complex impedance parameters of Pt–$As_2Te_{13}Ge_8S_3$–Pt quaternary glassy films stabilized via aging (or annealing) are extremely sensitive in adsorptive processes, so that even the presence of low reactive CO_2 in the ambiance can be detected at room temperature. The significant decrease in the frequency-dependent real and imaginary parts of the impedance during the adsorption of nitrogen dioxide is interpreted in terms of effective chemisorption processes, while the weak effects of both water and carbon dioxide vapors are attributed to their physisorption.

Acknowledgments. This work was supported by the National Agency for Research and Development of Moldova under Grant PS 20.80009.5007.21.

References

[1] R. Fairman and B. Ushkov, Eds., Semiconducting Chalcogenide Glass III. UK, Oxford, Academic Press, Elsevier, 2004 (R. Kwillardson and E.R. Weber, Series Eds., Semiconductors and Semimetals, vol. 80).
[2] J. R. Macdonald, Impedance spectroscopy, Wiley, New York, 1987.
[3] D. Tsiulyanu, T. Marian, A. Tiuleanu, et al., Thin Solid Films 517, 2820 (2009). http://dx.doi.org/10.1016/j.tsf.2008.11.073
[4] S. Sen, K. P. Muthe, N. Joshi, et al., Sens. Actuators, B 98, 154 (2004). http://dx.doi.org/10.1016%2Fj.snb.2003.10.004
[5] D. Tsiulyanu, M. Ciobanu, and O. Mocreac, Impedance Characterization of Gas Sensitive Chalcogenide Films, In: P. Petkov, D. Tsiulyanu, C. Popov, and W. Kulisch, Eds., Advanced Nanotechnologies for Detection and Defence against CBRN Agents, Springer, Dordrecht, 2018, pp. 317–332. http://dx.doi.org/10.1007/978-94-024-1298-7_31
[6] J. Greyson, Carbon, Nitrogen and Sulfur Pollutants and Their Determination in Air and Water, Marcel Dekker Inc., New York, 1990. https://doi.org/10.1002/jlcr.2580310110
[7] A. Haeusler and J.-U. Meyer, Sens. Actuators, B 34, 388 (1996). http://dx.doi.org/10.1016/S0925-4005(96)01847-3
[8] N. G. Patel, C. J. Panchal, and K. K. Makhija, Cryst. Res. Technol. 29, 1013 (1994).
[9] R. R. Desai, D. Lakshminarayana, P. B. Patel, and C. J. Panchal, Sens. Actuators, B 107, 523

(2005). http://dx.doi.org/10.1016/j.snb.2004.11.011
[10] D. Tsiulyanu and M. Ciobanu, Glass Phys. Chem. 45, 53 (2019). http://dx.doi.org/10.1134/S1087659619010140
[11] N. F. Mott and E. A. Davis, Electron Processes in Non-Crystalline Materials, Oxford Clarendon Press, Oxford, 1979.
[12] M. Kastner and H. Fritzsche, Philos. Mag. 37, 199 (1978). https://doi.org/10.1080/01418637808226653
[13] M. Ciobanu and D. Tsiulyanu, Chalcogenide Lett. 15, 19 (2018).
[14] J.-P. Kleider, J. Alvarez, A. Brézard-Oudot, et al., Sol. Energy Mater. Sol. Cells 135, 8 (2015). https://doi.org/10.1016/j.solmat.2014.09.002
[15] S. I. Marian, D. I. Tsiulyanu, and H.-D. Liess, Sens. Actuators, B 78, 191 (2001). https://doi.org/10.1016/S0925-4005(01)00811-5
[16] V. Georgieva, M. Mitkova, P. Chen, et al., Mater. Chem. Phys. 137, 552 (2012). https://arxiv.org/ftp/arxiv/papers/1204/1204.0444.pdf
[17] K. Pang, Y. Wei, W. Li, et al., Sci. China Technol. Sci. 63, 1566 (2020). https://doi.org/10.1007/s11431-020-1616-9
[18] D. Tsiulyanu, S. Marian, and O. Mocreac, Mold. J. Phys. Sci. 1, 264 (2012).
[19] T. Volkenstein, Electronic Processes on Semiconductor Surfaces during Chemisorption, Consultants Bureau Division of Plenum Publishing Co., New York, 1987.